Interpretation of seismic anisotropy in terms of mantle flow when melt is present

E Kaminski

Interpretation of seismic anisotropy in terms of mantle flow when melt is present

E. Kaminski

Institut de Physique du Globe de Paris and Université Paris 7 – Denis Diderot, Paris, France

Received 23 August 2005; revised 2 November 2005; accepted 7 December 2005; published 20 January 2006.

[1] The use of seismic anisotropy to image upper mantle flow is usually based on the assumption that the direction of fast propagation of seismic waves is the same as the flow direction. Laboratory experiments showed that when melt is present, it is rather the direction of slow propagation that aligns with the flow direction. This paper presents a modeling of the effect of melt on the development of lattice preferred orientation (LPO) and its implications for the interpretation of anisotropy. Taking into account strain partitioning associated with melt segregation in the modeling yields a good agreement with experimental results. Implementing strain partitioning in a test flow shows that the effect of melt is mainly local and has a limited effect on seismic anisotropy. Water-induced texture, melt-filled cracks or channelized flow, might better account for seismic observations of direction of fast propagation normal to plate motion on a regional scale. **Citation:** Kaminski, E. (2006), Interpretation of seismic anisotropy in terms of mantle flow when melt is present, *Geophys. Res. Lett.*, *33*, L02304, doi:10.1029/2005GL024454.

1. Introduction

[2] If isotropic seismic tomography gives a first order estimate of the repartition of density anomalies and thus of buoyancy forces in the mantle, only seismic anisotropy brings some constraints on mantle flow [*Montagner*, 1994; *Fouch and Fischer*, 1996; *Kendall and Silver*, 1996; *Savage*, 1999; *Park and Levin*, 2002]. Under the assumption that anisotropy in the upper mantle is due to lattice preferred orientation (LPO) of anisotropic minerals (mainly olivine) in the convective flow [*Nicolas and Christensen*, 1987], a model is required to link the evolution of LPO to the characteristics of the flow [*Tommasi et al.*, 2000; *Kaminski and Ribe*, 2002; *Blackman et al.*, 2002]. Two models of LPO development by plastic deformation include the effect of dynamic recrystallization [*Wenk and Tomé*, 1999; *Kaminski and Ribe*, 2001]. Amongst them, D-Rex, the one proposed by *Kaminski and Ribe* [2001], has been able to reproduce the results of laboratory experiments for simple shear and uniaxial compression of dry and wet olivine polycrystals [*Kaminski*, 2002; *Kaminski et al.*, 2004].

[3] Recently, new shear experiments performed in partially molten olivine aggregates [*Holtzman et al.*, 2003] have produced a puzzling LPO in which the slow (c-)axes rather than the fast (a-)axes align with the shear direction. This texture, which is the same as the type B LPO obtained for wet aggregates at high stress [*Jung and Karato*, 2001], casts some doubt on the direct use of seismic anisotropy as a proxy for mantle flow direction.

[4] Three different mechanisms can potentially explain the effect of melt on the development of LPO in a polycrystal. First, melt may change the activity of the slip systems, as does water at high stresses, so that c-slip is easier than a-slip, which yields a type B LPO. Second, strain partitioning associated with melt segregation between melt-free lenses and melt-rich bands, may be the kinematic origin of the texture. Last, a change in the physics of dynamics recrystallization could account for the observed LPO. *Holtzman et al.* [2003] interpreted their experiment in terms of strain partitioning, but they do not quantitatively address the implications for the mantle. This paper presents a quantitative test of this assumption and illustrates its consequences for the interpretation of seismic anisotropy in partially molten regions of the mantle.

2. Modeling of Texture Evolution in Presence of Melt

[5] A complete discussion of the experiments of [*Holtzman et al.*, 2003] is beyond the scope of this paper. Its aim is rather to use the experimental results to propose a quantitative test of the influence of melt on the interpretation of seismic anisotropy and of its relationship with mantle flow. To do so, a theoretical model (D-Rex) is used to reproduce the experimental results and then to extrapolate them to the convective upper mantle.

[6] D-Rex is a model of plastic deformation and dynamic recrystallization in an olivine polycrystal [*Kaminski and Ribe*, 2001]. It requires three sets of parameters (Table 1): an imposed deformation (specified or calculated from the flow), the resolved reference shear stress (i.e., strength) of each slip system, and the parameters of dynamic recrystallization (namely a dimensionless grain boundary mobility M^* and a dimensionless nucleation efficiency λ^*.) The plastic deformation of a crystal is calculated from its Schmid tensor that gives the rate of shear on each slip system as a function of its strength and orientation [*Kaminski and Ribe*, 2001]. The deformation is maximum for the grains with their softest slip system favourably oriented, and minimum for the grains in which only the hardest slip system is active. The strain energy in the crystals is estimated as a function of a balance between their rate of deformation (that increases the strain energy) and the probability of nucleation (that resets the strain energy), which itself is an exponential function of the deformation rate and of λ^*. The rate of change of the volume fraction of a crystal is then given by the difference

0094-8276/06/2005GL024454

Table 1. Model Parameters[a]

	E_{11}	E_{22}	E_{33}	Ω_3	$\tau_{(010)[100]}$	$\tau_{(001)[100]}$	$\tau_{(010)[001]}$
Dry	$\lvert\dot{\epsilon}\rvert$	$-\lvert\dot{\epsilon}\rvert$	0	$-\lvert\dot{\epsilon}\rvert$	1	2	3
Wet	$\lvert\dot{\epsilon}\rvert$	$-\lvert\dot{\epsilon}\rvert$	0	$-\lvert\dot{\epsilon}\rvert$	3	2	1
Melt	0	$-\lvert\dot{\epsilon}\rvert$	$\lvert\dot{\epsilon}\rvert$	$-\lvert\dot{\epsilon}\rvert$	1	2	3

[a]The reference sets of parameters for a dry aggregate are taken from *Kaminski and Ribe* [2001], and from *Kaminski* [2002] for a wet aggregate. The characteristics of deformation for strain partitioning are based on the observations of *Holtzman et al.* [2003]. In the three cases the parameters of dynamic recrystallization are the same as in *Kaminski and Ribe* [2001] ($\lambda^* = 5$, $M^* = 50$.)

between its strain energy and the average strain energy in the aggregate. The grains with a larger strain energy shrink, whereas the grains with a smaller strain energy grow by grain boundary migration, at a rate proportional to M^*. Different values of the free parameters in the model D-Rex can be chosen to reproduce the experimental results obtained in the presence of melt by *Holtzman et al.* [2003], but only some of these values are going to be consistent with the experimental conditions.

[7] The sketch of Figure 1 describes the basic experimental setting used by *Holtzman et al.* [2003]. This setting has to be expressed as an analytical deformation to be used as an input parameter in the model. Basic deformation types can be described by a strain rate tensor E_{ij} and a rotation vector Ω_k. The bulk imposed deformation in the work by *Holtzman et al.* [2003] is a dextral simple shear (i.e., an incompressible plane strain deformation) given by $E_{11} = |\dot{\epsilon}|$ (lengthening along x_1), $E22 = -|\dot{\epsilon}|$ (shortening along x_2), and $\Omega_3 = -|\dot{\epsilon}|$. The corresponding LPO is shown in Figure 1 for a sheared sample of olivine and 4% MORB, together with the LPO predicted by the model for a dry aggregate of pure olivine deformed under the same conditions (which corresponds to the regular type A LPO). The orientations of both c- and a-axes are orthogonal between the two cases, and the input parameters of the model have to be changed to correct this discrepancy.

[8] The first hypothesis that can be made to account for the new texture is a modification of the physics of dynamic recrystallization. In the model, this corresponds to a change of the dimensionless grain boundary mobility M^* and nucleation parameter λ^* in the presence of melt. A previous study [*Kaminski and Ribe*, 2001] showed that only the value of λ^* can change the type of texture associated to a specified deformation, and that the value of M^* only changes the rate of evolution of the LPO. Values of λ^* larger than 3 yield a type A texture (i.e., a-axes aligned with the direction of shear) whereas a value of λ^* smaller than 3 favor hard orientations and may mimic a type B LPO [*Kaminski and Ribe*, 2001]. A systematic grid search has been performed to find the value of λ (from 0 to 6 with increments of 0.1) that yields a texture in which the c- rather that the a-axes were aligned with the shear direction. The value of M^* was then changed (from 0 to 150 with increments of 5) to try to refine the fit. The best attempt is shown in Figure 2 for $\lambda^* = 1.4$ and $M^* = 20$. As illustrated by Figure 2, it was not possible to align both the c-axes to the shear direction and the a-axes with the normal of the shear plane without generating additional peak orientations not observed in the experiments. The concentration of the crystallographic axes around the peak orientations is also sharper than in the experiments. The weakness of the hypothesis of a change in dynamic recrystallization is supported by the observation of *Holtzman et al.* [2003] that the texture is created in melt-depleted regions rather than in melt-rich bands, whereas the effect of melt on dynamic recrystallization - if any - should be stronger where the content of melt is larger. Furthermore, one may note that melt is usually supposed to increase the efficiency of nucleation and grain growth [*Boullier and Nicolas*, 1975], whereas the model requires a reduction of the rate of these two processes relative to the dry case ($\lambda^* > 5$, $M^* > 50$). From this first test, one can thus conclude that a change in the physics of dynamic recrystallization cannot account for the texture. In the following, the reference values of *Kaminski and Ribe* [2001] ($M^* = 50$ and $\lambda = 5$) will be used.

[9] The second hypothesis that could account for the observed LPO is a change in the dominant slip system. The three active slip systems in olivine are (010)[100], (001)[100] and (010)[001]. For dry olivine polycrystals, the softest slip system is (010)[100], whereas for wet olivine polycrystals, the softest slip system is (010)[001] [*Kaminski*, 2002]. In D-Rex, the relative activity of the slip systems is given by their dimensionless reference resolved shear stresses (RRSS). The softest slip system has a RRSS of 1 and the RRSS of the harder slip systems are larger than 1. As wet aggregates display also a type B LPO when subject to a simple shear, the values of the RRSS for wet

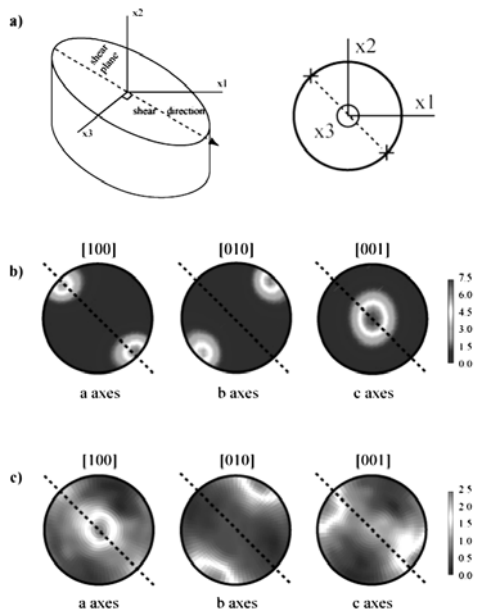

Figure 1. (a) Illustration of the experimental deformation and of the reference frame used in the model, in 3D and in the pole figures where the shear plane is shown as a dashed line and the shear direction is marked by crosses. (b) Pole figures (Lambert equal area projection, color scale corresponds to multiples of uniform distribution) of the LPO predicted by the model for a dextral simple shear ($E_{11} = -E_{22} = -\Omega_3 = |\dot{\epsilon}|$) and a deformation of 300% of a pure olivine aggregate (type A LPO). (c) Pole figures of the LPO observed in the experiments of *Holtzman et al.* [2003] for 300% shear of an aggregate of olivine +4% MORB (type B LPO).

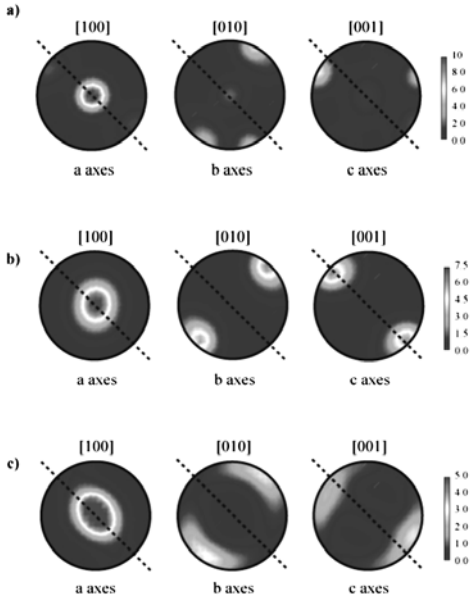

Figure 2. Pole figures of the LPO predicted by the model for a dextral simple shear for the three tested hypotheses. (a) Reduced efficiency of dynamic recrystallization ($\lambda^* = 1.4$, $M^* = 20$). The model prediction displays extra peak orientations that are not present in the experimental results. (b) Change of dominant slip system, from a slip to c slip. The bulk characteristics of a type B LPO are reproduced, but there is no back rotation of the peak orientation of b- and c-axes. (c) Strain partitioning as documented by *Holtzman et al.* [2003] (i.e., lengthening normal to the shear direction.) This hypothesis yields the best agreement with the experimental LPO as it reproduces a back-rotation of about 20 degrees of b- and c-axes.

olivine are first used (Table 1). The resulting LPO is shown in Figure 2. One key characteristic of the experimental texture is obtained: the a-axes lie on the shear plane and are normal to the shear direction, whereas the c-axes are aligned with the shear direction. However, the back-rotation of the b- and c-axes observed in the experiment is not reproduced in the model. To try to increase the fit between model and experimental LPO, the values of the RRSS of the three slip systems have been varied from 1 to 5 with increments of 0.1, but no value was able to produce a counter rotation. Furthermore, taking (010)[001] as the softest slip system implies that **c**-slip is easier than **a**-slip, and dislocations with a burgers vector parallel to the c-axis should be the most numerous in the samples. In their experiments, *Holtzman et al.* [2003] observe that dislocations with a burgers vector parallel to the a-axis are more numerous than dislocations with a burgers vector parallel to the c-axis, which is consistent with easier **a**-slip. The strength of this observation is relative because when dynamic recrystallization is active there is no straightforward relationship between the easiness of slip and the density of dislocations. The softness of a slip system tends to increase its related dislocation density, but a high density of dislocations increases the probability of nucleation that in turn highly reduces the density of dislocations. Additional measurements taking into account the status of each grain (relic or newly nucleated grain) and its orientations (or more precisely its Schmid factor) may yield a more definitive conclusion on the dominant slip. As a last point, one may also again note here the observation of *Holtzman et al.* [2003] that the texture is created in melt-depleted regions rather than in melt-rich bands, whereas the effect of melt on easiness of slip - if any - should be stronger where the content of melt is larger. Thus a change of activity of the slip systems induced by melt is not the best candidate to account for the experimental texture.

[10] The last test considers the hypothesis of strain partitioning favoured by *Holtzman et al.* [2003]. In their experiment, *Holtzman et al.* [2003] observe a lengthening of the sample normal to the shear direction associated with the segregation of melt. In the reference frame defined in Figure 1, this strain partitioning corresponds to a change of the direction of extension, from x_1 to x_3. Accordingly, the analytical expression of the deformation becomes $E_{22} = -\dot{\epsilon}$, $E_{33} = \dot{\epsilon}$ and $E_{11} = 0$. The rotation vector, which is controlled by the geometry of the apparatus, keeps the same expression $\Omega_3 = -\dot{\epsilon}$. The resulting LPO due to that strain partitioning is shown in Figure 2. Not only the bulk characteristics of the LPO are reproduced (a-axes normal to the shear direction and c-axes aligned with the shear direction) but also a back-rotation of about 20 degrees of the b- and c-axes is reproduced. Only the intensity of the peaks is somewhat larger in the model than in the experiments. This reflects that the bulk LPO in the sample is an average of zones affected by strain partitioning (displaying type B LPO), and unaffected zones (displaying type A LPO), which dilutes the total peak orientations.

[11] In conclusion, it appears that if a change of the activity of the slip systems could account for the bulk characteristics of the experimental LPO, only strain partitioning can reproduce the back-rotation of b- and c-axes which is of kinematic origin. Furthermore, the hypothesis of strain partitioning is the only one fully consistent with the observations of *Holtzman et al.* [2003]. Additional experimental constraints, such as the rate of evolution of the LPO with increasing strain, will make possible a refinement of the predictions of the model and may allow a better quantification of the respective role of the different parameters in the development of the texture. At the present stage, the agreement between the experimental results and the model predictions is however good enough to allow some extrapolation to the Earth's mantle in order to qualitatively infer its implications for seismic anisotropy.

3. Implications for the Mantle

[12] Partial melting occurs on specific and restricted portions of the Earth's upper mantle, typically at ridges, hot spots and subduction zones. Furthermore, the pressure gradients that drive liquid extraction from the melting zones induce significant melt focusing [e.g., *Spiegelman and McKenzie*, 1987]. The type B LPO directly associated to the segregation of melt is thus probably generated on a local scale only. The key question is then to infer if localized melt may leave a lasting imprint on the LPO carried out by the flow and should be taken into account in the interpretation of seismic anisotropy on a regional scale. This is relevant in particular for the regions where the fast polarization axis is

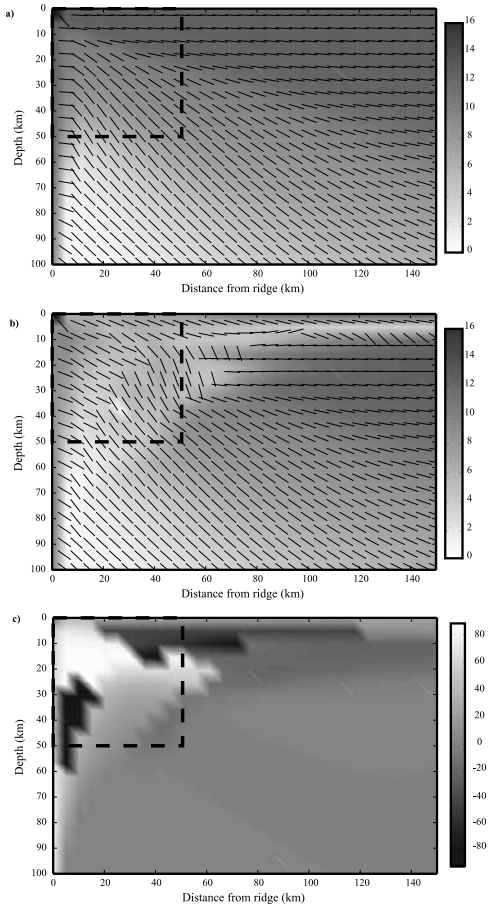

Figure 3. Seismic anisotropy of the medium with hexagonal symmetry that best fits the full elastic tensor predicted by D-Rex for a corner flow (note that the hexagonal symmetry is not fully valid close to the vertical axis.) (a) Dipping angle of the axis of fast propagation (bars) and percentage of anisotropy (grey scale) for a dry aggregate. (b) Same plot as in (a) but with strain partitioning taken into account when melt is present (square delimited by the dashed lines.) The percentage of anisotropy is reduced in the molten region. (c) Azimuthal orientation of fast propagation axis (in degrees) for the case with strain partitioning. Fast axes tend to be normal to the flow plane in the molten region.

normal to the direction of plate motion (mainly at mid oceanic ridges and in subduction zones [*Savage*, 1999]). To estimate the influence of melt on the LPO development, in a simple but qualitative way, a canonical corner flow is used to model a ridge flow. The depth of the model is set to 200 km and the zone where melt is present is set to a 50 $\times$ 50 km^2 square for the sake of the argument. In the calculation strain partitioning is supposed to affect all the grains (whereas in reality only the lenses with a low melt fraction will display a type B LPO), so this test flow gives an upper bound.

[13] The reference frame for the corner flow is such that x_1 is the horizontal direction parallel to the plate motion, x_3 is the vertical axis and x_2 is the horizontal direction normal to the flow plane. At each point in the corner flow, a strain rate tensor is defined as $E_{ij} = (\partial V_i/\partial x_j + \partial V_j/\partial x_i)/2$ where V_i is the flow velocity. When melt is present, strain partitioning is incorporated in the calculation by taking a different strain rate tensor, E^*_{ij}, defined as $E^*_{2i} = E^*_{i2} = E_{1i}$ and $E^*_{1i} = E^*_{i1} = E_{2i}$ for $i = (1, 2, 3)$. The results of the calculation are shown in Figure 3 as the anisotropy of the medium with hexagonal symmetry that best fits the full elastic tensor predicted by D-Rex as in *Kaminski et al.* [2004].

[14] The presence of melt has two significant effects on anisotropy. (1) First, the percentage of anisotropy decreases in the molten region. This is due to the fact that the crystals rotate from a (dry) type A LPO to a type B LPO due to strain partitioning. Because the direction of fast propagation is orthogonal between the two types LPO, the average anisotropy is diluted when the two LPO coexist. (2) Second, the orientation of the fast propagation axis rotates in the molten region. Not only the azimuth of the anisotropy tends to be normal to the flow plane, but the anisotropy is also vertically tilted. These two effects, though significant, occur mainly in the zone where melt is present and do not interfere with anisotropy away from the zone. This is due to the efficiency of dynamic recrystallization that quickly erases the type B LPO along a flow line once the aggregate has left the molten region. Only a 10 km deep layer of low anisotropy persists below the plate; resolving this thickness would be challenging, and only possible with certain types of seismic waves.

4. Conclusion

[15] This paper presents a quantitative interpretation of the experimental textures obtained during shear deformation of molten rocks by *Holtzman et al.* [2003]. Comparison between experiments and model predictions show that strain partitioning is the best mechanism to account for the type B LPO associated with melt segregation. Additional experimental work will allow a better understanding of the mechanism of strain partitioning. In particular the texture resulting from strain partitioning could be used in association with further theoretical modeling of LPO to study the progressive evolution of the texture as a function of strain and as a function of the melt concentration.

[16] The assumption of strain partitioning has been extrapolated to a test corner flow to infer its implication for the convective upper mantle. It is found that even if melt has a large effect on anisotropy in the zones with high melt content, this effect does not interfere with anisotropy on a regional scale. In particular, melt may not be sufficient to account for fast shear waves direction normal to the direction of plate motion. Anisotropy induced by the presence of water in subduction zones [*Jung and Karato*, 2001], by melt-filled cracks in rift zones or at ridges [*Blackman and Kendall*, 1997; *Kendall et al.*, 2005], or by channelized asthenospheric flow under mid oceanic ridges [*Xue and Allen*, 2005; *Toomey et al.*, 2002], may play a larger role than melt-induced texture. This first order conclusion will have to be strengthened by more detailed studies focused on a given area and based on more realistic flows in which the effect of melt on rheology is also taken into account.

[17] **Acknowledgments.** This paper has been much improved thanks to an anonymous reviewer's comments. I would like to thank Ben Holtzman and David Kohlstedt very much for making their experimental

data available and for helping me to better understand and model strain partitioning.

References

Blackman, D. K., and J. M. Kendall (1997), Sensitivity of teleseismic body waves to mineral texture and melt in the mantle beneath a mid-ocean ridge, *Philos. Trans. R. Soc. London, Ser. A*, *355*, 217–231.

Blackman, D. K., H.-R. Wenk, and J.-M. Kendall (2002), Seismic anisotropy of the upper mantle: 1. Factors that affect mineral texture and effective elastic properties, *Geochem. Geophys. Geosyst.*, *3*(9), 8601, doi:10.1029/2001GC000248.

Boullier, A. M., and A. Nicolas (1975), Classification of textures and fabrics of peridotite xenoliths from South African kimberlites, in *Physics and Chemistry of the Earth 9*, edited by L. H. Ahrens, pp. 97–105, Elsevier, New York.

Fouch, M. J., and K. M. Fischer (1996), Mantle anisotropy beneath northwest Pacific subduction zones, *J. Geophys. Res.*, *101*, 15,987–16,002.

Holtzman, B. K., D. L. Kohlstedt, M. E. Zimmerman, F. Heildelbach, T. Hiraga, and J. Hustoft (2003), Melt segregation and strain partitioning: Implications for seismic anisotropy and mantle flow, *Science*, *301*, 1227–1230.

Jung, H., and S. Karato (2001), Water-induced fabric transitions in olivine, *Science*, *293*, 629–631.

Kaminski, E. (2002), The influence of water on the development of lattice preferred orientation in olivine aggregates, *Geophys. Res. Lett.*, *29*(12), 1576, doi:10.1029/2002GL014710.

Kaminski, E., and N. M. Ribe (2001), A kinematic model for recrystallization and texture development in olivine polycrystals, *Earth Planet. Sci. Lett.*, *189*, 253–267.

Kaminski, E., and N. M. Ribe (2002), Timescales for the evolution of seismic anisotropy in mantle flow, *Geochem. Geophys. Geosyst.*, *3*(8), 1051, doi:10.1029/2001GC000222.

Kaminski, E., N. M. Ribe, and J. T. Browaeys (2004), D-rex, a program for calculation of seismic anisotropy due to crystal lattice preferred orientation in the convective upper mantle, *Geophys. J. Int.*, *158*, 744–752.

Kendall, J.-M., and P. G. Silver (1996), Constraints from seismic anisotropy on the nature of the lowermost mantle, *Nature*, *381*, 409–412.

Kendall, J.-M., G. W. Stuart, C. J. Ebinger, I. D. Bastow, and D. Keir (2005), Magma-assisted rifting in Ethiopia, *Nature*, *433*, 146–148.

Montagner, J.-P. (1994), Can seismology tell us anything about convection in the mantle?, *Rev. Geophys.*, *32*, 115–138.

Nicolas, A., and N. I. Christensen (1987), Formation of anisotropy in upper mantle peridotites: A review, in *Composition, Structure and Dynamics of the Lithosphere-Asthenosphere System*, *Geodyn. Ser.*, vol. 16, edited by K. Fuchs and C. Froidevaux, pp. 111–123, AGU, Washington, D. C.

Park, J., and W. Levin (2002), Seismic anisotropy: Tracing plate dynamics in the mantle, *Science*, *296*, 485–489.

Savage, M. K. (1999), Seismic anisotropy and mantle deformation: What have we learned from shear wave splitting?, *Rev. Geophys.*, *37*, 65–106.

Spiegelman, M., and D. McKenzie (1987), Simple 2-D models for melt extraction at mid-ocean ridges and island arcs, *Earth Planet. Sci. Lett.*, *83*, 137–152.

Tommasi, A., D. Mainprice, G. Canova, and Y. Chastel (2000), Viscoplastic self-consistent and equilibrium-based modelling of lattice preferred orientation: 1. Implications for the upper mantle seismic anisotropy, *J. Geophys. Res.*, *105*, 7893–7908.

Toomey, D. R., W. S. D. Wildcock, J. A. Conder, D. W. Forsyth, J. Blendy, E. M. Parmentier, and W. C. Hammond (2002), Asymetric mantle dynamics in the MELT region of the East Pacific Ridge, *Earth Planet. Sci. Lett.*, *200*, 285–287.

Wenk, H.-R., and C. Tomé (1999), Modelling dynamic recrystallization of olivine aggregates deformed in simple shear, *J. Geophys. Res.*, *104*, 25,513–25,527.

Xue, M., and R. M. Allen (2005), Asthenospheric channeling of the Icelandic upwelling: Evidence from seismic anisotropy, *Earth Planet. Sci. Lett.*, *235*, 167–182.

E. Kaminski, Équipe de Dynamique des Systèmes Géologiques, Institut de Physique du Globe de Paris, 4 Place Jussieu, F-75252 Paris cedex 05, France. (kaminski@ipgp.jussieu.fr)